


Microstructure and Mechanical Properties of AZ31/SiC and AZ31/CNT Composites Produced by Friction Stir Processing

A. Alavi Nia¹  · S. H. Nourbakhsh¹

Received: 22 April 2015 / Accepted: 25 August 2015 / Published online: 21 December 2015
© The Indian Institute of Metals - IIM 2015

Abstract Magnesium is a light structural metal that is increasingly used in the aerospace and automobile industries. Its mechanical strength can be enhanced by adding reinforcing particles to the material. Friction stir processing, a solid state process has been used to insert reinforcing particles into the structure of a material to create a composite with improved properties. In the present study, 4, 8 and 16 % (v/v) SiC nanoparticles or carbon nanotubes (CNT) were added to AZ31 alloy using FSP with simultaneous cooling and the microstructure, micro-hardness and tensile strength of the composites were examined. The results indicated that the addition of reinforcing materials decreased the size of the grains and increased structural uniformity and micro-hardness. SiC nanoparticles were distributed uniformly within the material; however, the CNTs agglomerated. It was found that increasing the percentage of reinforcing material increased the yield stress of the material, but decreased the ultimate stress and deformation.

Keywords Friction stir processing · Magnesium alloy · Mechanical strength · SiC · Carbon nanotubes

1 Introduction

Magnesium is one of the lightest structural metals and is used in industries such as aerospace and automobile industries because it is low density and has high specific

resistance [1]. There is a continuous attempt by the researchers to improve the mechanical resistance of magnesium using procedures such as friction stir processing (FSP).

FSP is a solid state method that changes the microstructure of materials. In this process, a rotating instrument composed of a shoulder and a pin is inserted into a specimen and moved in the desired direction at a fixed traverse and rotational speed. The material simultaneously moves from in front of the pin to behind it, which exposes the materials to high strain and extrusion strain rates and initiates dynamic recrystallization.

Studies on FSP of metals such as aluminum and magnesium indicate that it changes the mechanical properties of a material by changing its microstructure [2–6]. The success of FSP has motivated researchers to use it to add reinforcing particles to the structure of a material and examine the resulting mechanical properties. Dolatkhan et al. [7] added SiC particles (50 nm and 5 μm in size) to Al-5052 using FSP. They observed that decreasing the size the SiC particles and increasing the number of FSP passes decreased the size of the aluminum grains and the micro-hardness and wear properties of the resulting composite.

Salehi et al. [8] created Al6061 composite using 50 nm SiC particles. They reported that an increase in rotational speed and a decrease in traverse speed produced the best composite. They also found that a threaded pin performed better than a square pin. Choi et al. [9] uniformly distributed SiC particles in Al6060-T4 using FSP.

Researchers had also tested carbon nanotubes (CNTs) as reinforcing particles. Johannes et al. [10] produced a composite with a matrix of aluminum 7075 and reinforcing phases of CNT using FSP. The results showed that the CNTs were not damaged during FSP and indicated that the process could be used successfully to add CNTs to metals.

✉ A. Alavi Nia
alavi1338@yahoo.com; alavi495@basu.ac.ir

¹ Department of Mechanical Engineering, Bu-Ali Sina University, Hamedan, Iran

Esawi et al. [11] added different percentages of CNTs to aluminum powder. After mixing and milling, the powder was subjected to cold pressing and hot extrusion. They used FSP on the extrusion powder and found composites containing more than 2 % (v/v) CNTs experienced no change in ultimate stress from the non-uniform distribution of the nanotubes.

Liu et al. [12] distributed CNTs in aluminum using powder metallurgy and FSP. They showed that ultimate stress decreased and yield stress increased as the percentage of CNTs increased. Izadi and Gerlich [13] achieved uniform distribution of CNTs in AL5059 using multiple passes of FSP in a specific region. They reported that, damage to the CNTs increased as the number of FSP passes increased. Liu et al. [14] added different percentages of CNTs to Al1016 using five FSP passes and found that increasing the percentage of CNTs in the matrix increased the yield and ultimate stress. They attributed these results to the uniform distribution of the CNTs.

Previous studies included addition of nanoparticles to Al₂O₃ [15, 16] and a composite of B₄C and TiC to aluminum [17] to study the resulting wear properties and microstructure of the composites. In other studies reinforcing particles were added to magnesium, including Morisada et al. [18], who added 1 μm SiC particles to an AZ31 alloy. They reported that addition of the SiC particles increased the micro-hardness and decreased the grain size.

Najafi et al. [19] created a composite of 4 μm SiC particles in a matrix of AZ31. Their results indicated that the contiguous introduction of SiC particles and cooling during FSP resulted in a decrease in the size of the magnesium grains and increase in micro-hardness after recrystallization. Asadi et al. [20] added 5 μm SiC particles to AZ91 alloy and also observed that addition of SiC decreased grain size and increased the micro-hardness. In another study, Asadi et al. [21] introduced either Al₂O₃ or 30 nm SiC particles to an AZ91 alloy and reported that the SiC particles increased the micro-hardness and mechanical properties over the Al₂O₃ particles because of the tendency of the Al₂O₃ particles to agglomerate.

Sun et al. [22] used 40 nm SiC particles to fabricate a composite using an AZ63 alloy matrix. Their results suggested that SiC particles increased the micro-hardness, ultimate stress, and elongated the material; however, elongation of FSP samples with and without powder did not change.

Much less research has focused on the addition of CNTs to magnesium. Morisada et al. [23] added CNTs to AZ31

alloy and studied the microstructure and micro hardness of the composite. They reported that CNTs decreased grain size and increased the micro-hardness of the composite. Lu et al. [24] used different percentages of Al₂O₃ and CNTs in an AZ31 matrix to investigate the micro-hardness and wear properties of the resulting composites. Jiang et al. [25] employed SiO₂ nanoparticles in an AZ31 alloy to study the microstructure and micro-hardness of the composite.

A literature review revealed that few researchers have added reinforcing particles to AZ31 alloy to study their effect on the mechanical properties of the composite. The present study investigated the addition of 4, 8 and 16 % (v/v) SiC reinforcing particles or CNTs to AZ31 alloy using FSP on the microstructure, micro-hardness and tensile strength of the samples. To maintain a uniform distribution of reinforcing particles in the base metal, the traverse speed was kept low and rotational speed was high. Rapid cooling was used during the process to prevent an excessive increase in temperature.

2 Materials and Methods

The chemical composition of the AZ31 magnesium alloy is provided in Table 1. The magnesium specimens were machined to dimensions of 10 × 10 cm and a thickness of 10 mm. SiC particles with an average size of 50 nm and multi-walled CNTs 20–50 nm in diameter and 10–20 mm in length were used as additives, as shown in Fig. 1a.

Figure 1b shows the die used in the FSP, which consisted of a copper disk with coolant flowing through grooves embedded in it. This was used to control the rapid heat transfer between the coolant and the specimen. The water temperature was 10 °C and the flow rate for cooling was 1.5 lit/min. The diameter of the shoulder was 18 mm, the diameter of the pin was 7 mm, and pin length was 4 mm. The geometry of the pin was right-hand threaded with a pitch of 3 mm. The FSP was done with a rotational speed of 1000 rpm and a traverse speed of 28 mm/min (56, 48, 36 and 28 mm/min were chosen and finally 28 mm/min produced visually better results than others) The AZ31 sample was placed on the disk; heat transfer from the pin to the back of the plate in the first phase decreased the heat generated during FSP [26]. Four consecutive passes were performed.

The 4, 8, and 16 % (v/v) reinforcing materials were added to AZ31. Three grooves 1 mm in width and 1, 2 and 4 mm depth were created on the surface of the specimen.

Table 1 Chemical composition of AZ31 specimen

Mg	Al	S	Cl	K	Ca	Mn	Fe	Cu	Zn
95.5	2.82	0.056	0.18	0.041	0.023	0.42	0.011	0.0045	0.94

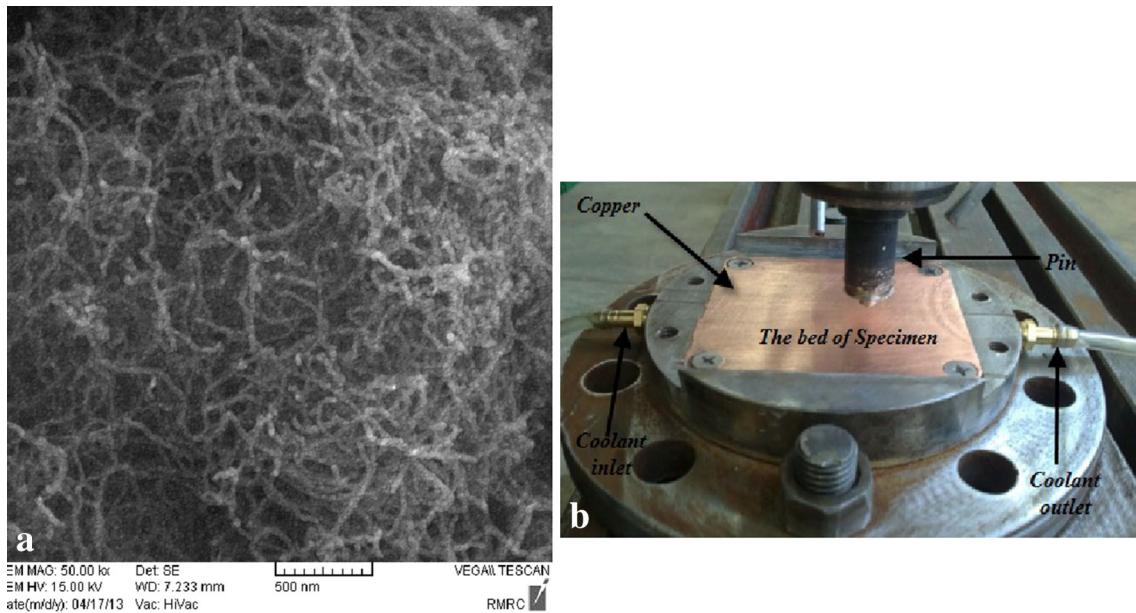


Fig. 1 a Carbon nanotubes, b the die used in the FSP process

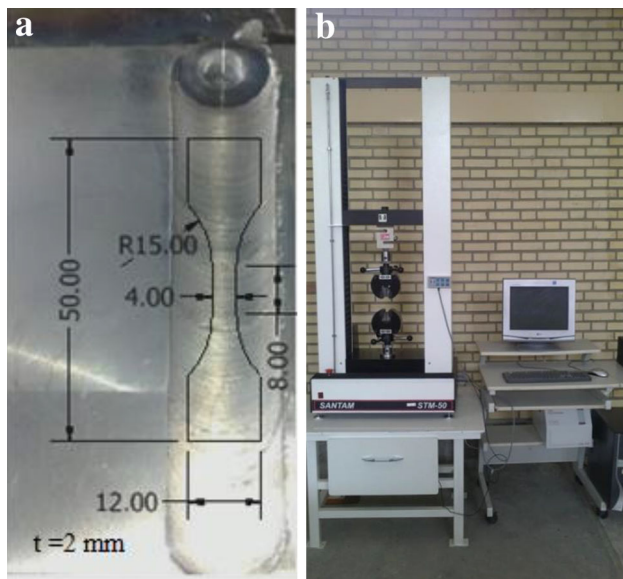


Fig. 2 a Tensile specimen dimensions, b tensile testing machine

The grooves were filled with the reinforcing phase and the surface was sealed using an instrument without a pin to avoid forcing the reinforcing materials from the grooves. FSP was carried out using an instrument with a pin in four consecutive passes with 100 % overlap in conjunction with cooling.

Tension test specimens were cut using electrical discharge machining and polished to eliminate surface resistance and other effects. The size and dimensions of the specimens were scaled based on a conventional standard

Table 2 The values of yield stress, ultimate stress and ductility

	Yield stress (MPa)	Ultimate stress (MPa)	Elongation (%)
Base	110.14	251.80	22.82
Without additive-1 Pass	56.71	267.35	33.01
Without additive-4 Pass	57.30	290.70	40.63
SiC-4 %	75.42	292.21	34.84
SiC-8 %	105.17	283.83	17.80
SiC-16 %	122.27	244.13	12.89
CNT-4 %	77.11	253.25	26.14
CNT-8 %	107.73	230.73	13.92
CNT-16 %	132.38	222.72	8.30

tensile specimen (Fig. 2a). Finite element analysis of the scaled tensile test was carried out to verify the specimen geometry without stress concentration effects. The thickness of the specimen was 2 mm. Tension tests were carried out at a strain rate of 0.01 in the FSP direction using a SANTAM 50 KN apparatus (Fig. 2b).

Micro-hardness of specimens were measured using a Buehler micro-hardness tester under 100 grf for 15 s. The surface of specimen was etched using a solution of 4.2 gr/gal picric acid, 10 ml acetic acid, 10 ml pure water, and 70 ml ethanol. A Union optical microscope and SEM were used to examine the microstructure of the specimens and the distribution of the reinforcing phase within the AZ31 alloy.

3 Results and Discussion

3.1 Microstructure

Figure 3 shows images from the optical microscope and Fig. 4 shows SEM images. The figure shows the microstructure of the base material (Fig. 3a), specimens without reinforcement (Fig. 3b), 4 % nanotubes (Fig. 3c), 4 % SiC nanoparticles (Fig. 3d), 8 % CNTs (Fig. 3e), 8 % SiC nanoparticles (Fig. 3f), 16 % CNTs (Fig. 3g), and 16 % SiC nanoparticles (Fig. 3h).

The base material shows a non-uniform structure with 18 μm grains. The average grain size of the AZ31 structure after four FSP passes and cooling was 6.4 μm without reinforcing materials, 3.08 μm with 4 % CNTs, 2.04 μm with 4 % SiC, 1.46 μm with 16 % CNTs, and 1.15 μm with 16 % SiC. Figure 3 shows that the SiC nanoparticles and CNTs decreased the size of the grains in the structure and made the structure more uniform. These results are similar to the findings of previous studies [7, 12, 18, 23]. Decreasing the linear speed of the FSP increased the size of the grains in materials with no reinforcing phase and in materials containing reinforcing particles in response to the extreme increase in specimen temperature. The reinforcing particles prevented a marked increase in the size of the grains, even at high temperatures [18].

Cooling during FSP prevented the excessive growth of grains. The distribution of 4, 8 and 16 % (v/v) SiC particles in the AZ31 alloy can be seen in Fig. 4a–c. As shown, as the percentage of SiC particles increased, they were increasingly scattered among the magnesium grains and were uniformly distributed. Similar results were reported elsewhere [18, 21, 22]. A uniform distribution of CNTs in the AZ31 alloy was not observed using SEM; Izadi and Gerlich [13] reported similar results for aluminum 5059. In their study, damage and deformation to nanotubes increased as the number of passes increased and, in some areas, agglomeration of nanotubes were observed.

EDS analysis detected a high percentage of carbon in the areas of interest, indicating a concentration of nanotubes. Figure 4a shows the average concentrations for three samples each at percentages of 4, 8 and 16 % (v/v) CNTs. The CNTs were relatively long and they easily entangled, which might have resulted in their undesirable distribution in the AZ31 alloy. Lim et al. [27] also observed that, after FSP, CNTs were entangled and not uniformly distributed throughout the aluminum matrix.

3.2 Micro-hardness

The micro-hardness increased as a result of three factors after the addition of reinforcing particles using FSP: fine

grain size, the percentage of reinforcing phases in the matrix, and quench hardening from the thermal expansion coefficient of the reinforcing particles and the matrix [7]. The micro-hardness of different samples is illustrated in Fig. 5. As seen, the micro-hardness increased from 67 Vickers for the base material to 108 Vickers for the composite with 16 % CNT and 112 Vickers for the composite with 16 % SiC. This can be represented as:

$$H_{\text{composite}} = H_{\text{matrix}}V_{\text{matrix}} + H_{\text{particle}}V_{\text{particle}} \quad (1)$$

where H is the micro-hardness and V is the volume (v/v). Figure 5 shows that the micro-hardness of the composite increased as the percentage of reinforcing phase increased [13]. This suggested that AZ31 alloy containing SiC nanoparticles displayed greater micro-hardness than AZ31 alloy containing CNTs.

An evaluation of the microstructure shows that a more uniform distribution of SiC nanoparticles in the matrix created a structure with a finer grain size that increased the micro-hardness of the composites. An increase in micro-hardness resulting from the uniform distribution of SiC nanoparticles was previously reported [16, 20]. The variation in micro-hardness of specimens containing CNTs were more uniform than in those containing SiC, which suggested the absence of uniform distribution of CNTs in the matrix. Lim et al. [27] reported non-uniform distribution of CNTs and micro-hardness. Morisada et al. [18, 23] explained that the micro-hardness of AZ31 alloy with CNTs was much greater than the alloy using 1 μm SiC nanoparticles, probably as a result of SiC nanoparticle size and the more uniform distribution of CNTs.

3.3 Tension Properties

The stress–strain curves for the base material with one pass and four passes of FSP without reinforcing particles and with 4, 8 and 16 % (v/v) SiC nanoparticles and CNTs are shown in Fig. 6. The numerical values for yield, ultimate stress, and ductility are listed in Table 2. The results for FSP without reinforcing particles revealed a decrease in yield stress and an increase in ultimate stress and ductility. Similar results were also observed by Mishra and Yuan [6] and Darras et al. [2].

Values for ductility and ultimate stress were greater for the material after four passes of FSP than after one pass because of the increased uniformity of the material structure and fine grain size. Venkateswarlu et al. [5] showed that three passes of FSP on AZ31 magnesium created a more uniform structure and increased ultimate stress and ductility. Figure 6a shows that the yield stress of the 4-pass FSP on AZ31 with SiC nanoparticles was greater than for

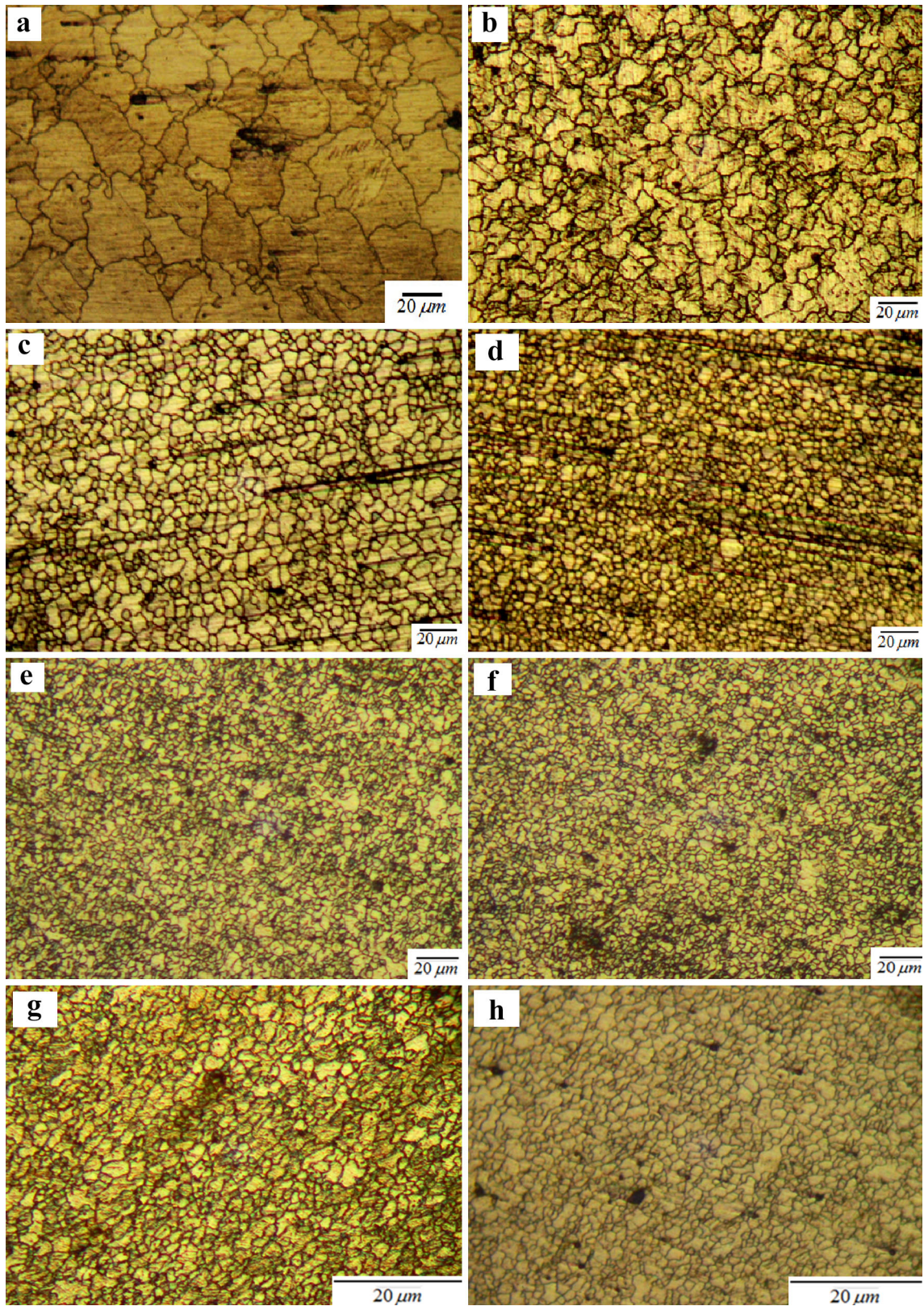


Fig. 3 The material texture in **a** the base material, **b** after four passes of FSP without reinforcing particles, **c** with 4 % CNT, **d** with 4 % SiC, **e** with 8 % CNT, **f** with 8 % SiC, **g** with 16 % CNT, **h** with 16 % SiC

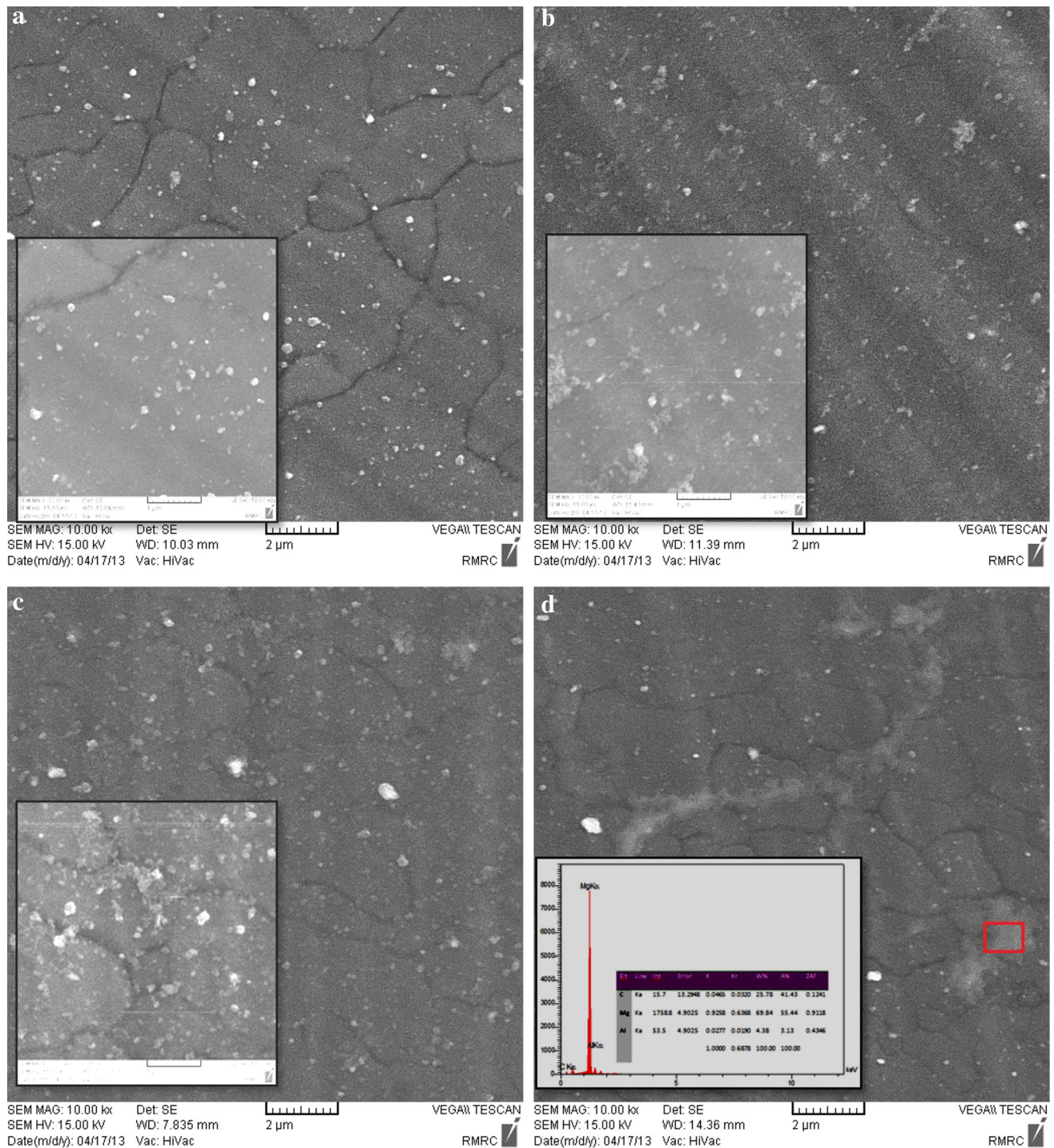


Fig. 4 a Distribution of 4 % SiC nanoparticles, b 8 % SiC nanoparticles, c 16 % SiC nanoparticle, d carbon nanotubes agglomeration within the AZ31 alloy

the same process without nanoparticles. Increasing the percentage of SiC nanoparticles increased the yield stress, but decreased the ultimate stress and elongation.

The increase in yield stress and decrease in elongation caused by the increase in the percentage of SiC nanoparticles was reported by Chawla and Shen [28]. SiC nanoparticles

reinforced the matrix using two mechanisms. In the first mechanism, the stresses were transferred from the matrix to the nanoparticles. The aspect ratio of the nanoparticles enhancing the strength of the composite from this mechanism was low, but it was reported that it had a specific influence on the increase in mechanical properties [28].

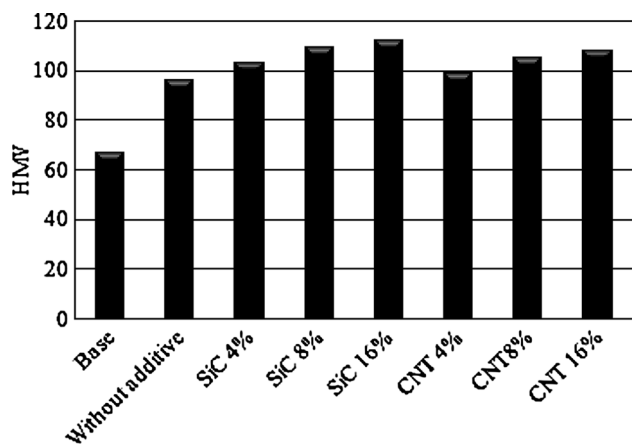


Fig. 5 Average values of micro hardness in the raw material, four times FSP process without reinforcing particle and composites contains 4, 8 and 16 percentages of SiC nanoparticles and carbon nanotubes

The second mechanism was that the difference between matrix and nanoparticle cooling initiated dislocations around the nanoparticles, but the nanoparticles prevented dislocation. In this way, the nanoparticles increased the strength of the composite [28]. The aspect ratio of the nanoparticles increasing the strength of the composite from this mechanism was low, but it was reported to result in a specific increase in the mechanical properties [28]. The properties of the composite made with 4 % SiC nanoparticles were the same as AZ31 without reinforcing particles. Sun et al. [22] reported that, when the amount of reinforcing particles was low, no increase in mechanical properties occurred.

Figure 4b shows the texture of the AZ31/CNT composite. As seen, an increase in the percentage of CNT increased the yield stress but decreased the ultimate stress and elongation. Other research indicated that increasing the percentage of nanotubes increased the yield and ultimate stress, but decreased elongation [14]. The researchers reported that the uniform or non-uniform distribution of nanotubes and the type of bonding between the nanotubes and matrix caused these differences in the results. The results of this research were consistent with that of Liu et al. [12].

The increase in yield stress for AZ31/SiC and AZ31/CNT can be numerically represented as:

$$\sigma_c = \left(\sigma_o + kd^{-1/2} \right) \left[V_f(s + 4)/4 + (1 - V_f) \right] \quad (2)$$

where σ_c is the yield stress of the composite, σ_o is the frictional stress caused by dislocation glide or an internal back stress, k is the Hall–Petch slope, d is the matrix grain size, v_f is the percentage of reinforcements, and s is the aspect ratio [12]. In this formula, the decrease in grain size and increase in percentage of nanoparticles increases the yield stress, which is consistent with the results of this study.

Table 2 shows that the yield stress for AZ31/CNT composite was greater than that for AZ31/SiC composite, especially for the 16 % specimen and was related to the aspect ratio. The aspect ratios for CNTs were larger than that for the SiC nanoparticles. Ultimate stress was more sensitive than yield stress to microscopic defects in the composite [15]. Large stress concentrations existed around the SiC nanoparticles and the two heads of the CNTs. This prevented the composites from releasing stress and caused

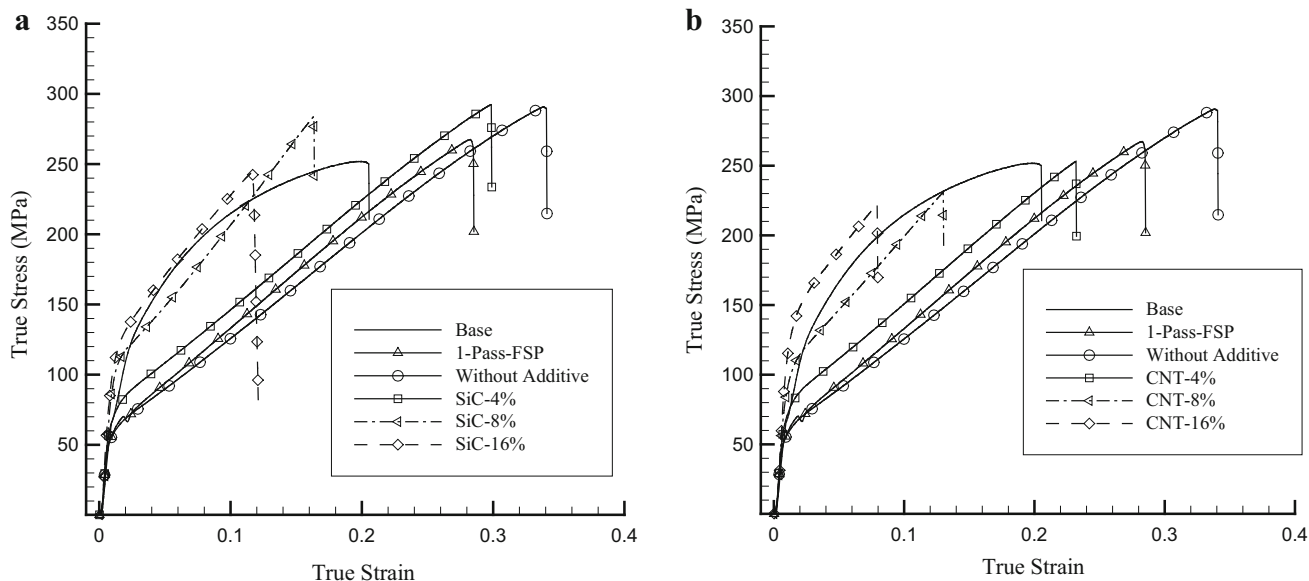


Fig. 6 Stress–strain curves of the raw material with one pass FSP process, four passes FSP process without reinforcing particles and with 4, 8 and 16 percentages of **a** SiC and **b** CNT

cracking. The composite, thus, could not bear large amounts of stress and the ultimate stress decreased. Increasing the percentage of reinforcing materials decreased the distance between them and made relaxation of the stress more difficult. This was another cause of the decrease in ultimate stress [12]. Agglomeration could decrease ultimate stress; Fig. 4 shows that the concentration of SiC nanoparticles increased as their percentage increased, resulting in a decrease in ultimate stress.

4 Conclusions

SiC nanoparticles and CNTs were added to AZ31 alloy using FSP. FSP was performed using one pass and four consecutive passes in conjunction with cooling. The microstructure, micro-hardness and tension properties of the base material were evaluated after one pass of FSP, after four passes of FSP without reinforcing particles, and after four passes of FSP after the addition of 4, 8 and 16 % (v/v) reinforcing materials. The main conclusions were:

1. FSP produced finer and more uniform grains. The uniformity increased and grain size decreased as the number of passes increased. The decrease in grain size improved the mechanical properties.
2. Adding SiC nanoparticles and CNTs prevented an increase in grain size and made the structure more uniform.
3. The micro-hardness of the material increased after FSP and the reinforcing phase.
4. SiC nanoparticles were more uniformly distributed in the AZ31 alloy than the CNTs after four passes of FSP.
5. The addition of reinforcing particles increased yield stress but decreased the ultimate stress and elongation.
6. Finally our results suggested that SiC nanoparticles were better reinforcement than CNT's for addition to AZ31.

Acknowledgments The authors are grateful for financial support from Iran National Science Foundation.

References

1. Mordike B L, and Ebert T, *Mater Sci Eng J* **302** (2001) 1.
2. Darras B, and Kishta E, *Mater Des J* **47** (2013) 133.
3. Pradeep S, and Pancholi V, *Mater Sci Eng J* **561** (2013) 78.
4. Ramesh K N, Pradeep S, and Pancholi V, *Metall Mater Trans A J* **43** (2012) 4311.
5. Venkateswarlu G, Devaraju D, Davidson M J, Kotiveerachari B, and Tagore G R N, *Mater Des J* **45** (2013) 480.
6. Yuan W, and Mishra R S, *Mater Sci Eng J* **558** (2012) 716.
7. Dolatkah A, Golbabaei P, Besharati Givi M K, and Molaiekiya F, *Mater Des J* **37** (2012) 458.
8. Salehi M, Saadatmand M, and Aghazadeh Mohandesi J, *T Nonferr Metal Soc J* **22** (2012) 5.
9. Choi D H, Kim Y I, Kim D A E U, and Jung S B, *T Nonferr Metal Soc J*, **22** (2012) 614.
10. Johannes L B, Yowell L L, Sosa E, Arepalli S, and Mishra R S, *Nanotechnol J* **17** (2006) 3081.
11. Esawi A M K, Morsi K, Sayed A, Taher M, and Lanka S, *Compos Part A Appl S* **42** (2011) 3.
12. Liu Z Y, Xiao B L, Wang W G, and Ma Z Y, *Carbon J* **50** (2012) 5.
13. Izadi H, and Gerlich A P, *Carbon J* **50** (2012) 12.
14. Liu Q, Ke L, Liu F, Huang C, and Xing L, *Mater Des J* **45** (2013) 343.
15. Mostafapour Asl A, and Khandani S T, *Mater Sci Eng J* **559** (2013) 549.
16. Zahmatkesh B, and Enayati M H, *Mater Sci Eng J* **527** (2010) 6734.
17. Rejil C M, Dinaharan I, Vijay S J, Murugan N, *Mater Sci Eng J* **552** (2012) 336.
18. Morisada Y, Fujii H, Nagaoka T, and Fukusumi M, *Mater Sci Eng J* **433** (2006) 50.
19. Najafi M, Nasiri A M, and Kokabi A H, *Int J Mod Phys B* **22** (2008) 2879.
20. Asadi P, Faraji G, and Besharati M K, *Int J Adv Manuf Technol* **51** (2010) 247.
21. Asadi P, Faraji G, Masoumi A, and Besharati M K, *Metall Mater Trans A J* **42A** (2011) 2820.
22. Sun K, Shi Q Y, Sun Y J, and Chen G Q, *Mater Sci Eng* **547** (2012) 32.
23. Morisada Y, Fujii H, Nagaoka T, and Fukusumi M, *Mater Sci Eng* **419** (2006) 344.
24. Hung F Y, Shih C C, Chen L H, and Lui T S, *J Alloys Compd* **428** (2007) 1.
25. Jiang Y, Yang X, Miura H, and Sakai T, *Rev Adv Mater Sci* **33** (2013) 29.
26. Chang C I, Du X H, and Huang J C, *Scr Mater J* **57** (2007) 3.
27. Lim D K, Shibayanagi T, and Gerlich A P, *Mater Sci Eng* **507** (2009) 194.
28. Chawla N, and Shen Y L, *Adv Eng Mater* **3** (2001) 357.